Fracture Toughness of HVOF Thermally Sprayed WC-12Co Coating in Optimized Particle Temperature

M. Jalali Azizpour*
Department of Mechanics, Ahvaz branch
Islamic Azad University, Ahvaz, Iran
E-mail: mjalali@iauahvaz.ac.ir
*Corresponding author

M. Salehi
Department of Materials Engineering,
Isfahan University of Technology, Iran
E-mail: surfacesalehi@hotmail.com

Received: 13 February 2017, Revised: 19 March 2017, Accepted: 18 April 2017

Abstract: In this paper the fracture toughness of WC-12Co coatings in optimum particle temperature in high velocity oxy fuel (HVOF) process have been studied by means of Vickers indentation. Multiple linear regression model applying Minitab, were used to determine the relationship and interaction between HVOF parameters and particle temperature. For genetic algorithm optimization, the signal to noise ratio was applied as a functional output of design of experiments. The results of validation test show a good agreement between obtained optimum condition and the results of genetic algorithm. The fracture toughness obtained by Vickers indentation shows the direct effect of particle temperature on coating toughness. The maximum amount of signal-to-noise using the genetic algorithm for velocity and temperature is 53.07 and -64.62, which equals 450.2 m/s and 1702^{o} C respectively. The results show that the Fracture toughness of WC-12Co deposited by LPG fuel in smallest level of temperature is $2.83 MPa(m)^{1/2}$ compared to $1.32 MPa(m)^{1/2}$ in highest temperature. The spray watch diagnostic system, micro-hardness test, Vickers indentation, X-Ray diffraction, EDS and scanning electron microscopy have been used for this purpose.

Keywords: Fracture toughness, Genetic algorithm, HVOF, WC-Co, S/N

Reference: Jalali Azizpour, M., Salehi, M., "The Fracture Toughness of HVOF Thermally Sprayed WC-12Co Coating in Optimized Particle Temperature", Int J of Advanced Design and Manufacturing Technology, Vol. 10/ No. 2, 2017, pp. 109–120.

Biographical notes: M. Jalali Azizpour received his PhD in Mechanical Engineering from Babol University of Technology in 2013. He is currently Assistant Professor at the Department of Mechanical Engineering, Ahwaz University, Ahwaz, Iran. His current research interest includes manufacturing and surface engineering. **M. Salehi** is Professor of Materials engineering at the Isfahan University of Technology, Iran. He received his PhD in Materials engineering from University of London, UK. His current research focuses on plasma spray and HVOF coatings.

1 INTRODUCTION

Coatings obtained by High velocity oxy fuel thermal spraying has found a special place due to its unique advantages, modified surface characteristics and very good resistance to wear and corrosion in oil, gas, petrochemical and aerospace. This approach is a good alternative to the traditional method of hard Cr-plating electrolyte that may lead to environmental risks and hazards [1], [2]. Tungsten-cobalt carbides (WC-Co) and tungsten carbide-nickel (WC-Ni) are widely used to prevent wear and corrosion. The findings of different researchers show that the wear resistance of WC-Co coatings deposited by HVOF thermal spraying is much more than the coating of chromium bath. In thermal spraying processes, residual stress can significantly be created during the process in the result of high thermal and kinetic energy and also because of different thermo-physical properties of the powder material and the substrate. In HVOF thermal spraying the final state of residual stress is a superposition of quenching, thermal mismatch and peening stresses.

Generally liquid fuel such as kerosene or gas fuels such as liquefied petroleum gas (LPG) or Propane are used in the HVOF equipment. Independent variables in HVOF method include the type of fuel, the ratio of fuel to oxygen, pressure and gas flow inlet, the nozzle diameter, powder feed rate, morphology and particle size distribution, carrier gas pressure, the speed of the gun and the gun distance from the surface of the substrate which determines the velocity and temperature of the powder particles in impact which ultimately affects the coating properties. The spray temperature can lead to phase degradation into phases with lower fracture toughness and in other side the spray velocity can generate peening action which is beneficial for residual stress and fatigue life [1-4]. The advantages of HVOF compared to other thermal spray processes are higher velocity, lower temperature and consequently lower thermal stresses, higher peening action and low levels of porosity.

Compressive residual stresses in the thermal coating have a beneficial effect on the fatigue behavior and coating adhesion. Fatigue and debonding of the coating are two main types of coating failure. Consequently, the evaluation of the cracking of coatings is important, which can ensure the reliability of coating. Many researches have been made on the methods of evaluation of the bonding strength and many methods have been attempted such as micro indentation, scratching and tension tests as well as simulation method in prediction of adhesion [5-7]. As the adhesive strength of WC-Co coating of HVOF thermally sprayed coating is higher than glue adhesion strength, so the tension test does not give a quantitative comparison in mechanical properties of these coatings [8]. Micro-indentation and nano-indentation techniques have commonly been used for measuring the mechanical properties of bulk materials, such as hardness, Young's modulus, and fracture toughness [9-11]. Recently, these techniques have been further developed and used for evaluating the adhesion strength of coatings or films to the substrate [12-15]. Mohammadi et al., [16] examined the adhesion and cohesion of plasma sprayed hydroxyapatite coatings on Ti-6Al-4V substrate using Vickers indentation. For this purpose, the Vickers indenter causes cracks in the coating and coating-substrate interface. The critical load with no crack was obtained by means of indentation. The results showed that increasing the energy and standoff leads to increasing the young modulus and fracture toughness of coatings. Chivavibul et al., [17] studied the effects of both carbide size and cobalt content on the properties of the coatings. It was found that the hardness and fracture toughness of the coatings were different from those of the sintered WC-Co. This discrepancy could be mainly explained by the hardening of the binder phase due to the dissolution of WC and the formation of amorphous/nanocrystalline phases. P. Chivavibul, et al., [18] studied the properties of WC-Co by JP5000 HVOF (kerosene fuel) system and the have reported fracture toughness of 4.2 MPa $(mm)^{1/2}$ and 10 $MPa(mm)^{1/2}$ for kerosene fuel HVOF and bulk WC-Co respectively.

In present research the genetic algorithm has been used to evaluate the optimum velocity and temperature of WC-12Co particles. Design of Experiments using standard Taguchi method and considering main parameters-spray distance, the ratio of oxygen to fuel gas, powder feed rate and movement speed gun- has been done for this purpose. The optimum conditions for spraying were obtained using the capability of MATLAB in genetic algorithms coding. In order to measure the particle velocity, optical system was used for monitoring the inflight particles. The fracture toughness of HVOF thermal spraying coating has been evaluated using Vickers indentation and Knoop micro-indentation. The major advantage of this methodology is that it does not require using any adhesive glue such as in tensile test.

2 MATERIALS AND METHODS

All The WC-12Co powder (HC Starck Co., Germany) with spherical particles shape and size of 15-45 μm was used. Normal distribution diagram of purchased powder size provided by supplier shows that the most of particles have 25 μm diameter. Chemical

composition of the used powder in weight% was: Co: 11.83%, C tot: 5.39%, C free: < 0.02%, Fe: <0.01% and W: Balance. Hipojet high velocity oxy fuel system with liquefied petroleum gas (LPG) fuel with flow rate of 70 ±10 l/min was used for this purpose. The powder feed rate and carrier gas flow rate were selected to be 38 g/min and 25 l/min respectively. The main process parameter and levels are given in table 1. Spray Watch diagnostic system (Oseir, Finland) was used for monitoring the particle velocity and temperature. X-ray diffraction with Kα-Cu and Scanning electron microscopy (SEM) were used to determine the composition and morphology of the powder respectively. Linear regression equation was obtained base on Taguchi methodology and signal to noise ratio analysis. Consequently, the optimum condition of particle velocity was obtained using the genetic algorithms in MATLAB codes. The micro-hardness of coating was measured according to ASTME384-10 in cross section of coating-substrate. The fracture toughness of coatings was evaluated by Vickers indentation.

Table1 Factors and levels

	Factor	Level
A	Stand off	3levels
B	O/F ratio	3levels
C	Feed rate (g/min)	2levels
D	Gun travel speed (m/s)	2levels

3 RESULTS AND DISCUSSION

A) SEM studies of powder and coatings

Fig. 1 shows scanning electron microscopy image of the morphology of WC-12Co powder particles. Most of powder particles are in spherical structure. Compared to other morphologies, the spherical particles need less kinetic energy to bond to the substrate [19]. Fig. 2 illustrates a general view of the coating after metallographic preparation. The WC-12Co HVOF thermally sprayed coating appears to be quiet dense. The presence of lamella boundaries, pores and equiaxial WC grain of different size embedded in the Co matrix is apparent.

B) Design of experiment

Spray Watch system was used to measure the temperature and velocity of the powder particles. For the measurement of velocity that is about 10.5 microseconds required to catch the particle. During this short time, the particles depending on their size pass a distance of 5.0 to 5.1 mm which is of 60-20 pixels on the CCD camera. By measuring the length of the path of the inflight particles, their velocity is achieved. Particle velocity differs according to particle size distribution. Taguchi approach has been used in order to designing, conducting as well as evaluating the effect of main spraying parameters on the impact velocity of particles in the HVOF thermal spraying process. The standard Taguchi array (L_9) and signal to noise ratio (base on 50 replications) are tabulated in table 2. It is known that when the experiments are repeated in any experimental situation, the signal to noise ratio analysis is the best way to calculate the effect of deviation around the mean value. Signal to noise ratio for tests with replication at each position, applying the bigger the better (particle velocity) and the smaller the better (particle temperature) quality characterization, is calculated using formulas 1 and 2 respectively [20].

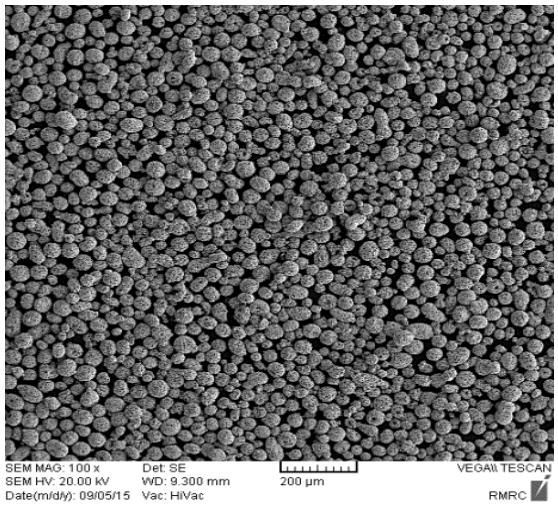

Fig. 1 SEM micrograph of WC-12Co powder particles

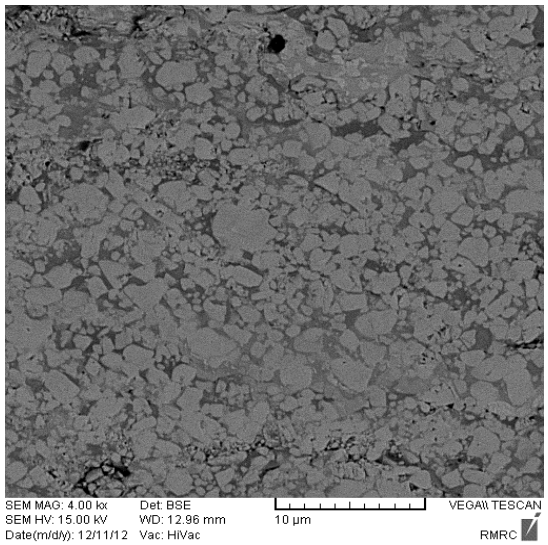

Fig. 2 SEM micrograph of WC-Co coatings

$$S/N = -10\log_{10}\left(\frac{1}{n}\sum_{i=1}^{n}\frac{1}{Y_i^2}\right) \quad (1)$$

$$S/N = -10\log_{10}\left(\frac{1}{n}\sum_{i=1}^{n}Y_i^2\right) \quad (2)$$

Which Y_i is the response of i-th replication.

Table 2 Applied array and S/N ratio

No.	A	B	C	D	S/N vel.	S/N temp. ˚C
1	170	2.5	38	1	52.81	-65.81
2	170	3.5	58	2	52.90	-66.25
3	170	4.3	38	1	53.05	-66.26
4	200	2.5	58	1	52.48	-65.38
5	200	3.5	38	1	52.91	-65.48
6	200	4.3	38	1	52.48	-65.94
7	250	2.5	38	2	52.40	-64.86
8	250	3.5	38	1	52.79	-65.37
9	250	4.3	58	1	52.47	-65.71

Fig. 3 illustrates the measured temperature distribution of powder with normal distribution of particle size for 4300 particles. Temperature of most of the particles is 2055.4˚C for a selected test situation. Figs. 4 and 5 illustrate the changes of S/N ratio at different levels of the study parameters. With the spraying distance increasing, particle velocity always reduces with a high gradient. The HVOF thermal spray system consists of a combustion chamber, converging-diverging nozzle, and a spraying gun tube. The reaction of fuel with oxygen generates a high thermal energy (enthalpy of combustion) in the combustion chamber. When the gas flows and expands through the converging-diverging nuzzle, it changes into kinetic energy, which increases gas velocity along the gun tube. The high velocity gas forms a supersonic free jet flow immediately when inter the free atmosphere. As density of the exiting gas is lower than the one of environment, a large volume of turbulent and low-velocity flow entrains into the jet from the surrounding air and reduces jet velocity in the spraying axis. The penetration rate of surrounding air into the jet intensifies and consequently the velocities of jet and particles reduce considerably with the distance between nozzle and substrate layer increasing. The LPG fuel used in this study is a combination of 70 percent butane and 30 percent propane. In HVOF combustion process, there are two main chemical reactions; the combustion of chamber, hydrogen and carbon with oxygen. For combustion the hydrogen with oxygen:

$$2H_2(g) + O_2(g) \rightleftharpoons 2H_2O(g) \quad (3)$$

$$H_2(g) + O_2(g) \rightleftharpoons 2OH(g) \quad (4)$$

And for carbon with oxygen:

$$2C(g) + O_2(g) \rightleftharpoons 2CO(g) \quad (5)$$

$$2CO(g) + O_2(g) \rightleftharpoons 2CO_2(g) \quad (6)$$

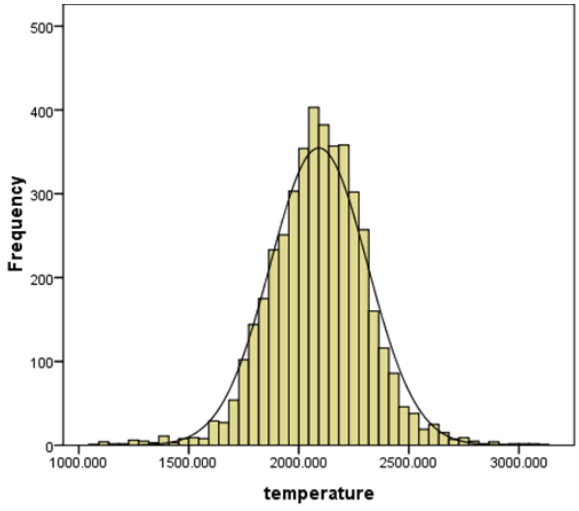

Fig. 3 Normal distribution of particle temperature

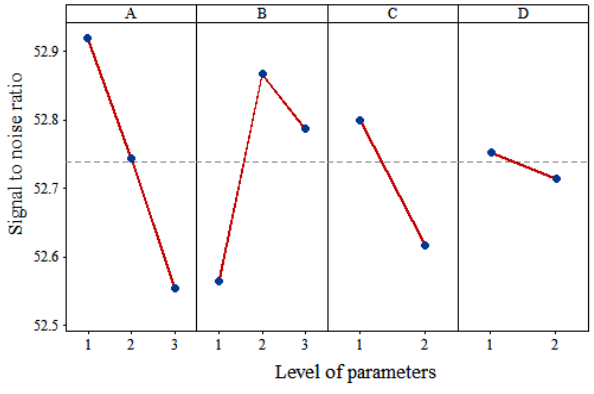

Fig. 4 S/N vs levels of parameters for particles velocity

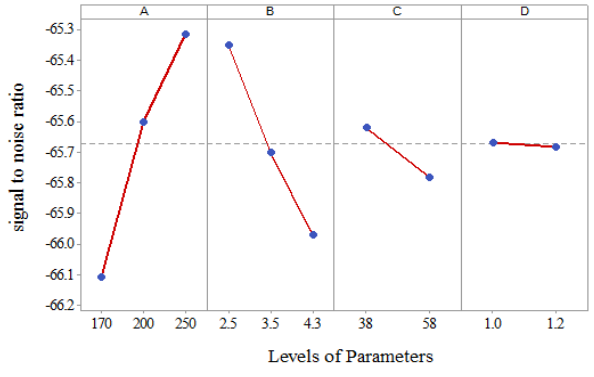

Fig. 5 S/N vs levels of parameters for particles temperature

In the modeling of HVOF thermal spray, it is important to note that because of high operating temperature, combustion products will dissociate into a number of species with low molecular weight, for example, CO, OH, and H [22, 23]. Under the general condition, combustion reaction of C_xH_y hydrocarbon with oxygen occurs as Eq. 7.

$$AC_xH_y + bO_2 \rightarrow cH_2O + dCO_2 + eCO + fO_2 + gH_2 + hOH + mH + nO \quad (7)$$

At all levels tabulated in Table 1, oxygen-to-fuel ratio is lower than the stoichiometric ratio (5.96 on molar basis). Temperature of combustion products increases with decreasing rate by increasing of the oxygen-to-fuel ratio up to stoichiometric mixture. Meanwhile, the particle velocity has increased with the oxygen-to-fuel ratio increasing up to the rate of 3.5 (lower than stoichiometric). Velocity decreases with this ratio increasing, which might be attributed to the presence of the species due to dissociation of combustion product components, especially CO. Dissociation reactions are endothermic. Therefore, some part of enthalpy of combustion is spent for dissociating of products with the oxygen-to-fuel ratio increasing, which reduces temperature of combustion gases.

In Table 3, it can be seen that the calculated flame composition changes as a function of flame temperature. An increase in temperature reduces combustion products and a decrease in temperature increases combustion products. It is important to note that the amount of free oxygen (O_2) is relatively small at low temperatures compared to the other species (H_2O and CO_2), but it increases when temperature is above 1500°C. Then it is expected that concentration and accumulation of molecules in combustion products increases with the increasing of oxygen-to-fuel ratio (temperature increase). Therefore, velocity of gas and particles reduced at the highest level of oxygen-to-fuel ratio (4.3).

Modeling phase of particles in an HVOF process is usually performed based on the Lagrangian approach. The average distance between individual particles in a dispersed two-phase flow (gas-solid) can be estimated using Formula 8 [25].

$$\frac{L_d}{d_p} = \left[\frac{\pi}{6}\frac{1+k}{k}\right]^{\frac{1}{3}} \quad (8)$$

Where L_d is the distance between two particles and k is the ratio of particle loading to particle/gas density ratio. L_d/d_p ratio in a two-phase flow with one dispersed phase should be greater than 10. Based on a particle loading of 4% and a density ratio of 10^3 to 10^4, L_d/d_p ratio is about 20 to 50, which implies that the individual powder particles are isolated from each other. Therefore, it is reasonable to assume that particle coalogution is negligible, and thus the powder size distribution does not change during flight.

With the powder feed rate increasing from level 1 to level 2, actually, distances between individual particles decreases and particle coalogution probability increases. Based on momentum principle sustainability (m_pv_p), it is expected that particle velocity would decrease with the particle mass increasing as shown by Figures 3 and 4, gun travel speed has no considerable effect on particle velocity; however, it may affect thermal stresses and bond strength due to the impact of warming coating and substrate during processing.

Table 3 The combustion product as mole percent (%) [24]

Temperature (°C)	1480	2030	2470	2800
Co_2(g)	49.75	44.94	30.7	16.77
H_2O(g)	49.87	47.52	39.33	27.86
CO(g)	0.1869	3.773	13.93	22.5
O_2(g)	0.1104	1.986	6.834	10.24
HO(g)	0.03185	0.9167	4.407	8.766
H_2(g)	0.05042	0.6941	2.548	4.821
O(g)	0.00025	0.07121	1.128	4.623
H(g)	0.00054	0.08284	1.077	4.369
OH(g)	0.001051	0.01246	0.0328	0.04351
HO_2(g)	4.871E-06	0.00035	0.00246	0.00523
C_2H_4(g)	5.097E-29	1.915E-23	1.078E-20	2.607E-19

C) Mathematical Modeling

The second order linear regression equations were used for the mathematical modeling for more accurate curve fitting of velocity and temperature as below respectively.

$$Y = \beta_0 + \sum_{i=1}^{p} \beta_i x_i + \sum_{i=1}^{p} \beta_{ii} x_i^2 + \sum_{i} \sum_{j \neq i} \beta_{ij} x_i x_j + \varepsilon \quad (9)$$

$$y = \beta_0 + \sum_{i=1}^{p} \beta_i x_i + \sum_{i} \sum_{j \neq i} \beta_{ij} x_i x_j + \varepsilon \quad (10)$$

The least square method is used, where all β coefficients are regression coefficients. X_i is the independent variable, p is number of variables, and y is the dependent variable. The Pearson correlation coefficient (Eq. 11) was used for further examination of the effect of parameters and their interactions. The closer the correlation coefficient is to values 1 and -1, the more suitable the linear relationship will be between parameters. If the coefficient is equal to zero or very close to zero, it will indicate lack of a linear relationship between two parameters [21].

$$R = \frac{\sum_{i=1}^{n}(x_i - \bar{x})(y_i - \bar{y})}{\sqrt{(\sum_{i=1}^{n}(x_i - \bar{x})^2 \sum_{i=1}^{n}(y_i - \bar{y})^2)}} \quad (11)$$

Where, (x_i, y_i) is ordered pair of " i" observation.
The results of Pearson correlation for particle temperature (Tables 4 and 5) show that the effect of parameter B is second order linear and the effect of parameters A and C is in first order linear form. Moreover, interactions A×C and A×D have the maximum effect on velocity. Parameter D and AXB, B×C, B×D, and C×D have no significant effect on output and they are considered as regression errors. As mentioned above, Equations 9 and 10 is summarized as Eqs. 12 and 13.

Table 4 Pearson correlation coefficient for parameters

	A	B	C	D
Linear Correlation	0.73	-0.59	-0.17	-0.02

Table 5 Pearson correlation coefficient for interactions

	A×B	A×C	A×D	B×C	B×D	C×D
Linear Correlation	-0.06	-0.27	0.67	-0.51	-0.58	-0.21

Table 5 Pearson Correlation Coefficient for interactions

$$S/N = \beta_0 + \beta_1 A + \beta_2 B + \beta_3 C + \beta_4 B^2 + \beta_5 AC + \beta_6 AD \quad (12)$$

$$S/N = \beta_0 + \beta_1 A + \beta_2 B + \beta_3 AD + \beta_4 BC + \beta_5 BD \quad (13)$$

Regression function is calculated after determining regression coefficients using the least squares error method and Minitab for particle velocity and temperature respectively (Eqs. 14 and 15).

$$S/N(V) = 50.702 + 0.00383A + 1.162B + 0.0184C - 0.1496B^2 - 0.00014AC - 0.00216AD \quad (14)$$

$$S/N(T) = -66.471 + 0.0056A + 0.013B + 0.0036AD - 0.00243BC - 0.227BD \quad (15)$$

Tables 6 and 7 show the results of regression analysis. To make comment on the accuracy of a regression equation, its coefficient of determination (R^2 و R_{adj}^2) is usually considered as a criterion. The values above R^2=99.16% and R_{adj}^2=99.62% show that the achieved regression equation is a suitable model for describing changes of spray velocity of powder particles in terms of the independent variables in Table 2.

D) Genetic Algorithm

In fact, genetic algorithm is a method for finding an approximate solution of optimization problems using the concepts of biology such as inheritance. In this algorithm, the variables are binary coded. Then using computer simulation of conservation laws, the weaker characters are replaced by more appropriate characters. This process is repeated to gain the best results. The process is iterated as long as the best response is achieved. The fundamental steps for analyzing optimization problems using genetic algorithm code writing are as follows:

1- Defining variables as a chromosome with a constant length, selecting size of a chromosome, determining crossover probability (P_c) and Mutation probability (P_m)

2- Defining a target function for assessing chromosomes

3- Generating population of primary chromosomes randomly

4- Assessing the selected population

5- Copying the best members in a new generation

6- Performing a crossover action for each pair of chromosomes (parents) and generating two new chromosomes (offspring)

7- Performing a mutation action for the selected chromosomes and generating mutated offspring

8- Creating a new generation (merging 5, 6, and 7)

9- Assessing the new generation

10- Returning to Step 5 in case termination condition is not satisfied [18].

Table 6 Regression analysis for velocity

Term	Coef	T-Value	P-Value
Constant	50.702	84.81	0
A	0.00383	0.68	0.568
B	1.162	2.69	0.115
C	0.0184	0.87	0.478
B*B	-0.1496	-2.28	0.15
A*C	-0.00014	-1.31	0.321
A*D	-0.00216	-1.85	0.205

This research aims at achieving the maximum (optimal) velocity of powder spray in a HVOF process. Genetic algorithm code writing in a MATLAB environment was used for this purpose. regression equations were

used as a target function for algorithm implementation. The algorithm structure was established by selecting a 20 binary population randomly with the string length of 64 bits (for each 16-bit independent parameter) as the primary population and considering probabilities of crossover and mutation as 80 percent and 10 percent, respectively.

Table 7 Regression analysis for temprature

Term	Coef	T-Value	P-Value
Constant	-66.471	-128.69	0
A	0.0056	0.39	0.72
B	0.013	0.02	0.988
A*D	0.0036	0.29	0.794
B*C	-0.00243	-1.18	0.322
B*D	-0.227	-0.3	0.781

A double point crossover method was used for generating two new offspring for each selected pair of chromosomes (parents). Figs. 6 and 7 show changes of signal to noise, which was calculated by the genetic algorithm. As the diagram shows, value of signal to noise remains constant after about 200 iterations and it converges on 53.07. When signal to noise ratio is used for analyzing optimization problems, the results achieved for estimating optimal conditions, should be converted into the primary units. The equivalent mean square deviation (MSD) is obtained from Eqs. (16 and 17) with the signal to noise ratio with "the more, the better" attribution. Table 8 shows the optimal conditions predicted by the genetic algorithm.

Table 8 Optimal condition predicted by GA

	A	B	C	D	S/N	Optimal
Velocity	170	3.9	38	1	53.07	450.2 m/s
Temperature	250	2.5	58	1.2	-64.62	1702º C

$$\mathrm{MSD} = \frac{1}{Y^2} = 10^{-\left(\frac{S/N}{10}\right)} \quad (16)$$

$$\mathrm{MSD} = Y^2 = 10^{-\left(\frac{S/N}{10}\right)} \quad (17)$$

E) Verification Test

A verification test was used for verifying the optimal results achieved by the genetic algorithm. Figure 8 and 9 show the verification test results for the tests with iteration, (exceeding 50 iterations), in the position predicted by the genetic algorithm. Mean of the optimal velocity of particles and signal to noise ratio were 446.5 m/s and 53, respectively.

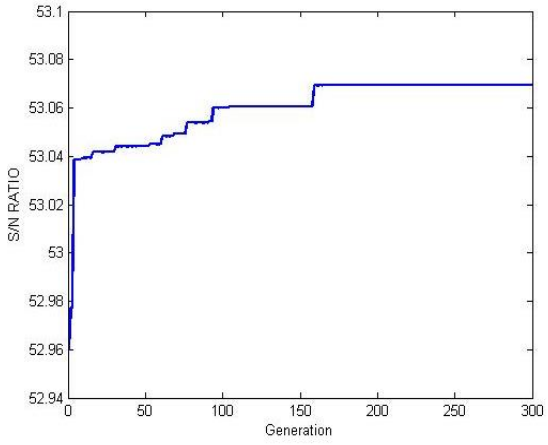

Fig. 6 Plot of Number of Generation Vs S/N Ratio (Velocity)

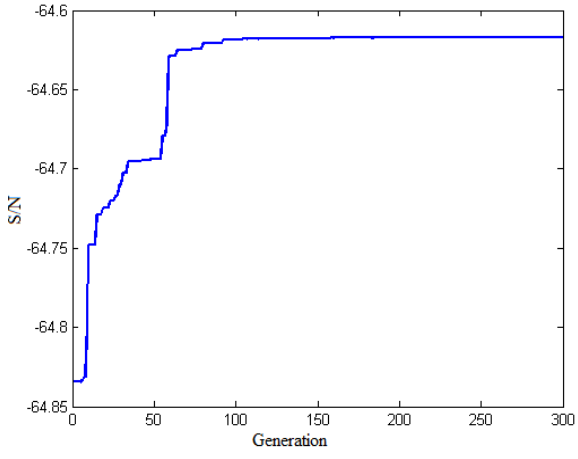

Fig. 7 Plot of Number of Generation Vs S/N Ratio (Temperature)

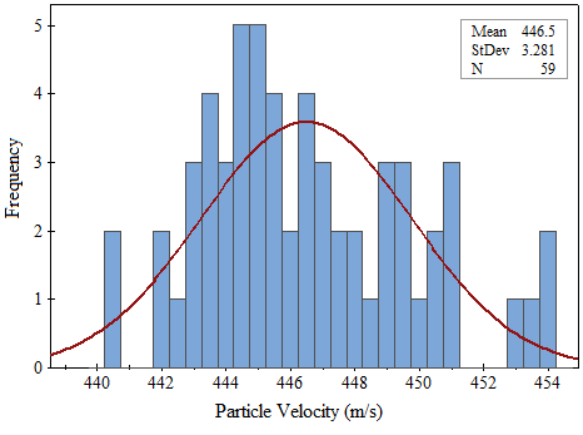

Fig. 8 Frequency distribution of powder velocity in verification test with 50 replications

In statistical issues, confidence interval is an approximate range for data, which is used for the reliability of an estimate. Confidence interval is obtained for the mean value of a set of data and

observations, C.I.(m), with a certain confidence level using the following equation [12].

$$C.I.(m) = E(m) \pm \sqrt{\frac{F_\alpha(f_1.f_2) \times V_e}{n_e}} \quad (18)$$

Where $F_\alpha(f_1, f_2)$ is the variance ratio, which is obtained by Table F at the confidence level of 1-α. F_1 is the mean degree of freedom, which is always equal to one, f_2 is the error degree of freedom, v_e is error variance, and n_e is number of equivalent responses.

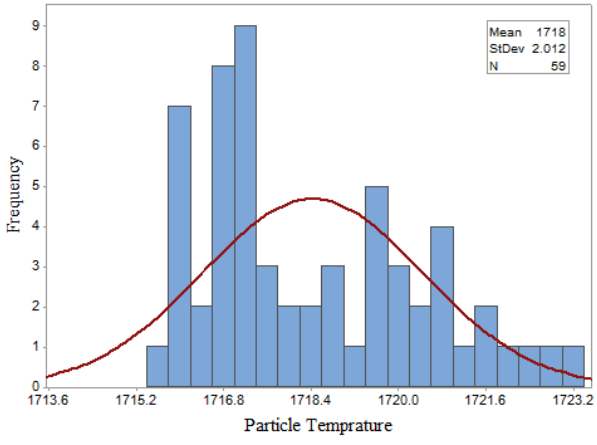

Fig. 9 Frequency distribution of powder temperature in verification test with 50 replications

The result of confidence interval calculation for velocity and temperature at the predicted levels are tabulated in table 9 and 10. The test result improves that the optimal velocity obtained from the test is compatible with the velocity predicted by the genetic algorithm.

Table 9 Confidence interval results for velocity

	GA	EXPERIMENT
SNR	53.07	53
Velocity (m/s)	450.2	446.5
C.I.	53.07±0.13	
	f_1=1, f_2=3, n_e=1.29, V_e=0.0022	

Table 10 Confidence interval results for temperature

	GA	EXPERIMENT
SNR	-64.62	-64.7
Temperature	1702	1718.5
C.I.	-64.62±0.34	
	f_1=1, f_2=3, n_e=1.29, V_e=0.0152	

F) ANOVA

ANOVA is one of the statistical applications, which examines the effect of variables on a response individually. In other words, ANOVA specifies contribution of the effect of each factor on output. Contribution percentage (P) for a specific factor is obtained from dividing total Net Square by sum of total squares.

Tables 11and 12 shows the ANOVA results based on the stated signal to noise ratio. The signal to noise ratio for 50 iterations in each test condition with "the more, the better" attribution was obtained. With approximately 48 percent of contribution, spray distance has the maximum effect on signal to noise ratio. Powder feed rate and oxygen-to-fuel ratio has 35 and 16 percent respectively. The effect of gun velocity parameter is slight and it is merged by the error parameter. After merging gun velocity factor, ANOVA error is 1.5 percent. For particle temperature the O/F ratio and gun travel speed have same contribution, but the spray distance have more effect on temperature (58.87%) rather than velocity (47.6%). Meanwhile the particle temperature is less affected by powder feed rate.

Table 11 ANOVA table for particle velocity based on S/R

factor	DF	SS	MS	F	P%
A	2	0.9683	0.4841	31.9	58.87
B	2	0.5798	0.2899	19.1	35.25
C	1	0.0512	0.0512	3.37	3.11
D	(1)	pooled			
Error	3	0.0455	0.0152		2.77
Total	8	1.6448			100.0

G) Fracture toughness

The most important limiting factor in the assessment of fracture toughness of WC-Co coatings applying Vickers indentation is, the relatively good toughness compared to ceramic coatings. Therefore, in order to have cracks the higher loads must be applied compared to ceramic coatings.

In addition, the Vickers indentation causes irregular cracks and some measurement problems in WC-Co coatings. The bulk WC-Co materials need loads higher than 50 Kgf for initiating the cracks and it depends on the amount of cobalt. Nevertheless, the WC-Co coatings can be evaluated at lower loads. Khameneh Asl et. al., [28] suggested at least load 18 Kgf to have an effective assessment in fracture toughness. Their results showed that the cracks in tungsten carbide cobalt coating deviate toward coating interface or free surface. For this purpose, more than10 indents in load range of 2-20 Kgf for each condition were used. Only 5 indents in each condition were applicable. Fracture toughness of coatings (KC) was determined by Vickers indentation method and following equation was used to obtain K_C [29]:

$$K_c = 0.016[\frac{P}{C^{3/2}}][\frac{E}{H}]^{1/2} \quad (19)$$

Where P is the applied load and C is the crack length ahead of diagonal of indentation and E is the elasticity modulus (Fig. 10). The micro-hardness of coatings was measured of 1225.5 and 835 for maximum and minimum temperature and the average elasticity modulus of 175GPa was used for WC-12Co coating in this study.

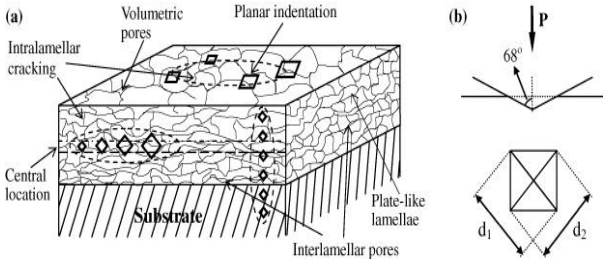

Fig. 10 Vickers indentation in cross section [30]

Fig. 11 shows the SEM morphology of the crack in both corners of indent in WC-12Co coating. The results of measurement of cracks lengths show that in maximum particle velocity and minimum particle temperature the fracture toughness are calculated of 1.32 MPa $(m)^{1/2}$ and 2.83 MPa$(m)^{1/2}$ respectively. P. Chivavibul, et al., [18] studied the properties of WC-Co by JP5000 HVOF (kerosene fuel) system and have reported fracture toughness of 4.2 MPa$(m)^{1/2}$ and 10 MPa$(m)^{1/2}$ for kerosene fuel HVOF and bulk WC-Co respectively. This may be attributed due to oxidation of WC and Co in higher temperatures in gas fuel HVOF which is discussed in next section. This is due to generation of hard brittle phases in LPG fuel HVOF with higher thermal energy in this study which is discussed in next section. For bulk cemented carbides, the fracture toughness is obtained at least 11.7 MPa $(m)^{1/2}$ for different cobalt content by S. Sheikh [31].

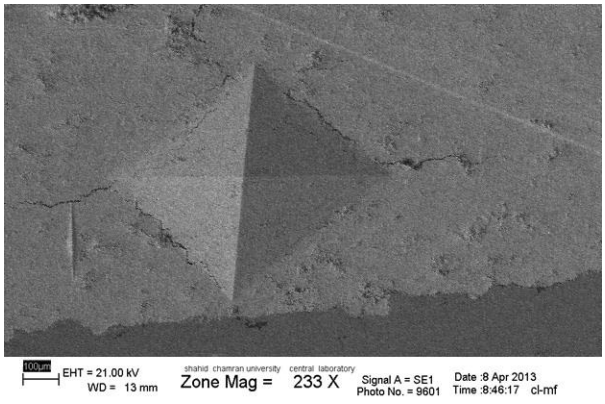

Fig. 11 Crack morphology (SEM image)

Diffraction patterns of powder and coating are shown in Fig. 12. The XRD analysis shows that the powder contains just WC and Co in particle composition. In condition of maximum particle velocity (smallest spray distance and biggest O/F), the particles also are at their maximum level of temperature. In such elevated temperatures, decomposition and oxidation of WC phase tends to be a problematic issue.

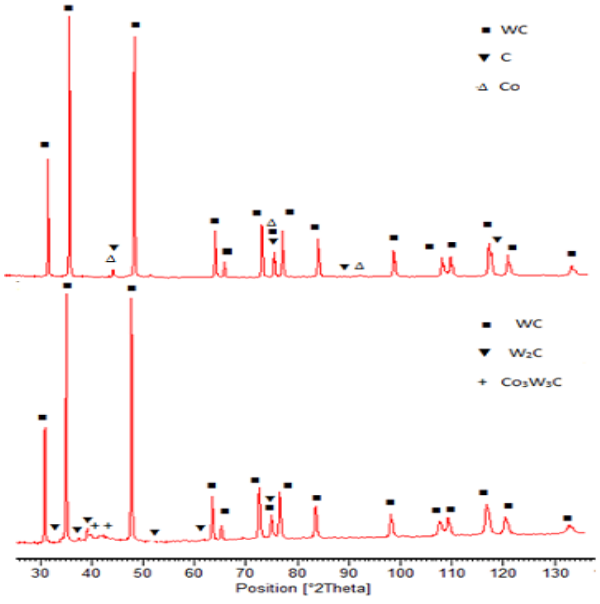

Fig. 12 XRD pattern of WC-12Co coatings

Table 13 shows the possible oxidation reactions and equivalent negative or positive Gibbs energies. In the solid state, several reactions can take place simultaneously. Reaction rates can vary for kinetic reasons, and is dependent on temperature, mass transfer in the reaction zone, oxygen partial pressure, etc.

In general, it can be concluded that solid-state oxidation is less important compared to the oxidation reaction in the liquid state, due to kinetic constraints. The high reaction rate requires solid-gas or liquid-gas reactions. Solid-solid reactions are too slow for the HVOF spraying process, as the spray particles are in reaction conditions less than 2ms. Thus, only the most probable reactions occur. The reactions are divided in two categories; reactions with pure oxygen, and reactions with carbon dioxide and water vapor. These are the main combustion products of HVOF spraying and are effective gases in the plume. The decarburization reaction has a high gibbs value, which means that the decomposition of WC is highly probable via this reaction, providing oxygen is available.

Fig. 13 illustrates the SEM micrograph of WC-12Co in this study. W_2C phase in the outer surface of WC (tungsten carbide border of the matrix) due to higher atomic mass than the WC is visible with bright colors. Vernon and Guilemany [32,33] have also reported epitaxial growth of W_2C on the WC crystal as shown in

Fig. 13. According to Gibbs energy provided in table 13, the most possible reaction is oxidation of WC to brittle W_2C phase (Eq. 20). As this form of oxidation is more active in higher temperature, it is reasonable to have more W_2C and consequently have a coating with lower fracture toughness.

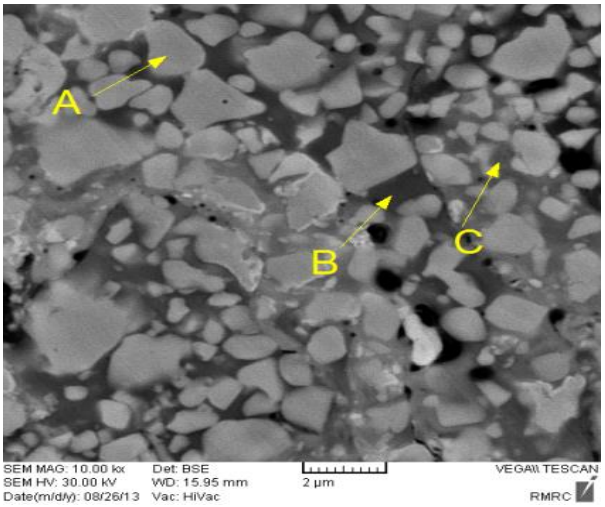

Fig. 13 SEM micrograph of WC-Co on 10Kx magnification

In WC-Co system the main reaction is decarburizing of WC phase. Carbon tendency to react with oxygen is much more than cobalt and tungsten and therefore the oxidation is of great importance. Given that the tungsten carbide are dispersed in cobalt matrix, during the spraying and cooling, the reactions below can help decomposition of WC. The remaining amount of carbon and tungsten present in the matrix creates a nano-crystal and amorphous phases with a grain size of less than 8 nm[24]. where [W] Co and [C] Co denote elements dissolved in the Co melt. Here, W_2C denotes forming of a W_2C layer by diffusion on a WC grain; WC and Co form a heterogeneous melt:

$$3Co+3WC+O_2 \rightarrow Co_3W_3C+2CO \quad (28)$$

$$12Co+12WC+5O_2 \rightarrow 2Co_6W_6C+10CO \quad (29)$$

Fig. 14 illustrates the results of EDS analysis of WC particles (area A), cobalt-rich (dark gray background B) and light gray background (area C). As it is clearly obvious, Area C has more tungsten and less cobalt in comparison with the area B. Zone B may include Co, Co_2C and is Co_3W_3C phase. In Area C due to the lower concentration of cobalt and lighter color than the area B, the heavier phases such as W-C-Co Co4W4C, Co_6W_6C and tungsten carbides such as $W_6C_{2.54}$ are more likely to create. All these phases have been identified in X-ray diffraction in this study.

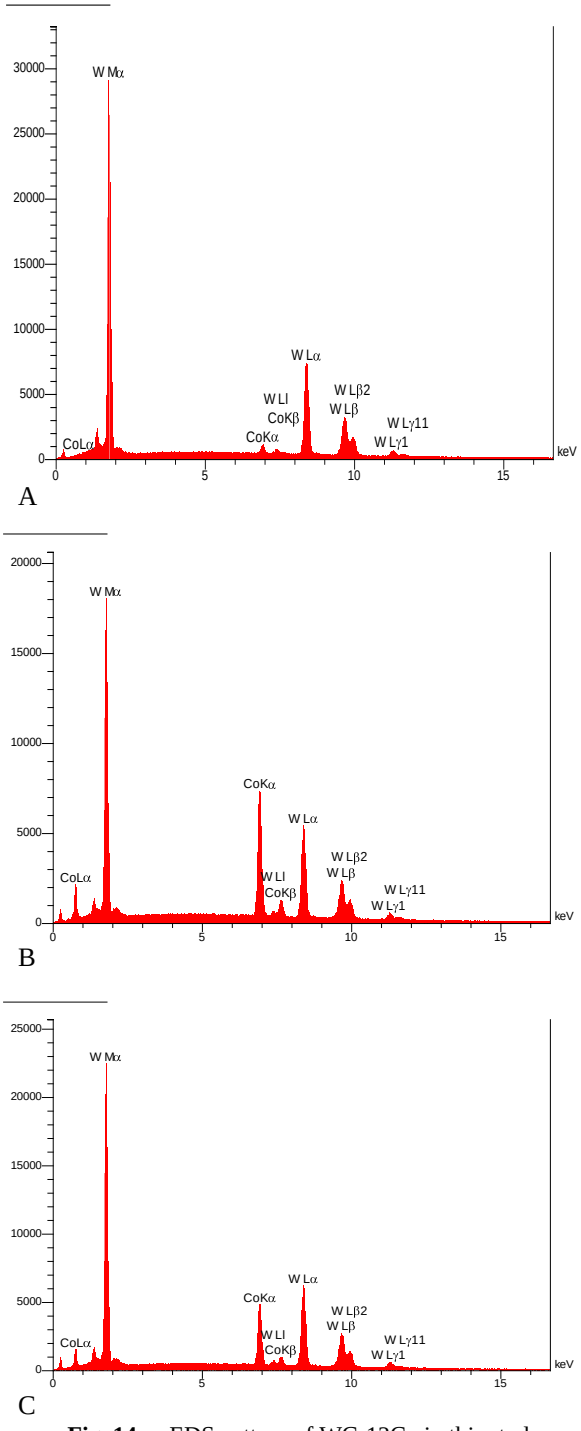

Fig. 14 EDS pattern of WC-12Co in this study

$$4WC + O_2 \rightarrow 2W_2C + 2CO \qquad \Delta_R G^{\circ} 1800℃ = -543\ kJmol^{-1} \quad (20)$$

$$2WC + O_2 \rightarrow W_2C + CO_2 \qquad \Delta_R G^{\circ} 1800℃ = -375\ kJmol^{-1} \quad (21)$$

$$2WC + O_2 \rightarrow 2W + 2CO \qquad \Delta_R G^{\circ} 1800℃ = -517\ kJmol^{-1} \qquad (22)$$

$$2WC + CO_2 \rightarrow W_2C + 2CO \qquad \Delta_R G^{\circ} 1800℃ = -168\ kJmol^{-1} \qquad (23)$$

$$2WC + H_2O \rightarrow W_2C + CO + H_2 \qquad \Delta_R G^{\circ} 1800℃ = -140 kJmol^{-1} \qquad (24)$$

$$W_2C + H_2O \rightarrow 2W + CO + H_2 \qquad \Delta_R G^{\circ} 1800℃ = -113 kJmol^{-1} \qquad (25)$$

$$2Co + O_2 \rightarrow 2CoO \qquad \Delta_R G^{\circ} 1800℃ = -172 kJmol^{-1} \qquad (26)$$

$$2/3W + O_2 \rightarrow 2/3WO_3 \qquad \Delta_R G^{\circ} 1800℃ = -231\ kJmol^{-1} \qquad (27)$$

4. CONCLUSION

The particle characterization and fracture toughness of HVOF thermally sprayed WC-Co coatings have been studied. A brief conclusion of findings is as below:

1- The maximum amount of signal-to-noise using the genetic algorithm for velocity and temperature is 53.07 and -64.62, which equals 450.2 m/s and 1702 ºC respectively.

2- Genetic algorithm is a powerful tool for searching optimal condition in a continuous interval between the minimum and maximum levels of the effective parameters in a problem. Therefore, the optimal amount of 3.9 was achieved for oxygen-to-fuel ratio using the genetic algorithm, which is not observed in all the levels defined in Table 1.

3- The Fracture toughness of WC-12Co deposited by LPG fuel in smallest level of temperature is 2.83 MPa$\sqrt{m}$ compared to 1.32 MPa$\sqrt{m}$ in highest temperature (biggest level of particle velocity).

REFERENCES

[1] Jalali Azizpour, M., Nourouzi, S., "Evaluation of Thorough Thickness Residual Stress in WC-Co Coating using Electro Discharge Hole Drilling Method", Iranian Journal of Surface Science and Engineering, 2012, pp. 9.

[2] Picas, J. A., et al., "Influence of HVOF Spraying Parameters on the Corrosion Resistance of WC–CoCr Coatings in Strong Acidic Environment", Surface and Coatings Technology, 2013, Vol. 225, pp. 47-57.

[3] Jalali Azizpour, M., Nourouzi, S., "Evaluation the Effect of Process Parameter on the Velocity of HVOF Thermally Sprayed WC-Co Particles", Iranian Journal of Surface Science and Engineering, 2012, pp. 6.

[4] Nourouzi, S., M. Jalali Azipour, and Salimijazi, H. R., "Parametric Study of Residual Stresses in HVOF Thermally Sprayed WC–12Co Coatings", Taylor & Francis Group, 2014, pp. 9.

[5] Aixin, F., Yongkang, Zh, Huakun, Xie., "Characterization of Interfacial Adhesion and Bond Strength Between thin Film Coating and Substrate by Scratch Testing", Journal of Jiangsu University (Natural Science Edition), Vol. 24, No. 2, 2003, pp. 15-18.

[6] Hua, Ch., Maozhong, Yi, and Kewei, Xu, "Bonding Strengths of PCVD Films under Cyclic Loading", J. Surface and Coatings Technology, 1995, Vol. 74, pp. 253-258.

[7] Eaton, H. E., Novak, R. C., "A Study of the Effects of Variations in Parameters on the Strength and Modulus of Plasma Sprayed Zirconia", Journal of Surface and Coatings Technology, Vol. 27, No. 3, 1986, pp. 257-267.

[8] ASTM C633-79 Standard "Test Method for Adhesion of Cohesive Strength of Flame-Sprayed Coatings", [S]. American Society for Testing and Materials, 1993.

[9] Oliver, W. C., Pharr, G. M., "Measurement of Hardness and Elastic Modulus by Instrumented Indentation: Advances in under-standing and Refinements to Methodology", J. Mater. Res., Vol. 19, 2004, pp. 3–20.

[10] Kruzic, J. J., Kim, D. K., Koester, K. J., Richie, R. O., "Indentation Techniques for Evaluating the Fracture Toughness of Biomaterials and Hard Tissues", J. Mech. Behav. Biomed. Mater. 2, 2009, pp. 384–395 (2009)

[11] Ranade, A. N., Krishna, L. R., Li, Z., Wang, J., Korach, C. S., and Chung, Y. W., "Relationship Between Hardness and Fracture Toughness in Ti-TiB2 Nanocomposite Coatings", Surf. Coat. Technol., Vol. 213, 2012, pp. 26–32.

[12] Drory, M. D., Hutchinson, J. W., "Measurement of the Adhesion of a Brittle Flm on a Ductile Substrate by Indentation", Proc. R. Soc. Lond. A 452, 1996, pp. 2319–2341.

[13] Chicot, D., Démarécaux, Ph., and Lesage, J., "Apparent Interface Toughness of Substrate and Coating Couples from Indentationtests", Thin Solid Films 283, 1996, pp. 151–157.

[14] Marot, G., Lesage, J., Démarécaux, Ph., Hadad, M., Siegmann, St., and Staia, M. H., "Interfacial Indentation and Shear Tests to Determine the Adhesion of Thermal Spray Coatings", Surf. Coat. Technol., Vol. 201, 2006, pp. 2080–2085.

[15] Qi, H., Yang, X., and Wang, Y., "Interfacial Fracture Toughness of APS Bond Coat/Substrate under High Temperature", Int. J. Fract., 157, 2009, pp. 71–80.

[16] Mohammadi, Z., Ziaei-Moayyed, A. A, Mehdi-Mesgar, A.S., "Adhesive and Cohesive Properties by Indentation Method of Plasma-Sprayed Hydroxyapatite Coatings", Journal of Appl. Surf. Sci., Vol. 253, 2007, pp. 4960-4965.

[17] Chivavibul, P., Watanabe, M., Kuroda, S., and Shinoda, K., "Effects of Carbide Size and Co Content on the Microstructure and Mechanical Properties if HVOF-Sprayed WC-Co Coatings", Surf. Coat. Technol., Vol. 202, No. 3, 2007, pp. 509-521.

[18] Chivavibul, P., Watanabe, M., Kuroda, S., "Effect of Powder Characteristics on Properties of Warm-Sprayed

WC-Co Coatings", Journal of Thermal Spray Technology, Vol. 19, No. 1-2, January 2010, pp. 81.

[19] Kamnis S., Gu S., "Study of In-Flight and Impact Dynamics of Nonspherical Particles from HVOF Guns", Journal of Thermal Spray Technology, Vol. 19, No. 1-2, January 2010, pp. 31-42.

[20] Ranjit, R., "A Primer on the Taguchi Method", Second ed. 1990, Society of Manufacturing Engineers.

[21] Borgnakke ,C., Sonntag, R. E., "Fundamentals of Thermodynamics", Seventh ed, 2009: Don Fowley.

[22] Li, M., Christofides, P. D., "Multi-scale Modeling and Analysis of an Industrial HVOF Thermal Spray Process", Chemical Engineering Science, Vol. 60, No. 13, 2005, pp. 3649-3669.

[23] Li, M., D. Shi, and Christofides, P. D., "Modeling and Control of HVOF Thermal Spray Processing of WC–Co Coatings", Powder Technology, Vol. 156, No. 2–3, 2005, pp. 177-194.

[24] Karpiola K., "High Temperature Oxidation of Metals, Alloys and Cermet Powders in HVOF Thermal Spraying", Doctoral thesis, Helsiniki University of Technology, 2004.

[25] Crowe, C. T., et al., "Multiphase Flows with Droplets and Particles". Second ed. 2012, Taylor & Francis Group, LLC.

[26] Bazargan, A., "Applied Linear Regression", Third ed. 2012: Shiraz University.

[27] Melanie M., "An Introduction to Genetic Algorithms, A Bradford Book the MIT Press Cambridge", London, England 5th Printing, 1999.

[28] Khameneh Asl Sh. "Study of the Effect of the Indentation Time and Load on Fracture Toughness and Crack Morphologies in WC-17Co Thermally Sprayed HVOF Coating", Materials Science Forum, Vol. 465-466, 2004, pp. 301-306.

[29] Ansatis, G. R., Chantikul, P., Lawn, B. R., and Marshall, D. B., "A Critical Evaluation of Indentation Techniques for Measuring Fracture Toughness: I, Direct Crack Measurement", Journal of the American Ceramic Society, Vol. 64, 1981, pp. 532-538.

[30] Zh. Yin, Sh. Tao, "Evaluating Microhardness of Plasma Sprayed Al_2O_3 Coatings using Vickers Indentation Technique", Journal of Physics D: Applied Physics, Vol. 40, No. 22.

[31] Sheikh, S., "Fracture Toughness of Cemented Carbides: Testing Method and Microstructural Effects", International Journal of Refractory Metals and Hard Materials, Vol. 49, March 2015, pp. 153-160.

[32] Guilmany J.M., Dosta S., Nin J., and Minguel J.R., "Study of Proerties of WC-Co nanostructured Coatings Sprayed by High Velocity Oxyfuel", Vol. 14,2005,405-412.

[33] Guilemay, J. M., Nutting, J., and De Paco, J. M., "Characterization of Three WC12Co Powders and the Coatings Obtained by High Velocity Oxy fuel Soraying", Proc, Fourth European Conf. Adv. Materials process, 1995, Assoc, Itallian Dimetallurgica, 1996, pp. 395-398.